THE PROTEIN SOCIETY

Remodeling of the conformational ensemble of the repeat domain of tau by an aggregation enhancer

Elias Akoury,[1] Marco D. Mukrasch,[1] Jacek Biernat,[2] Katharina Tepper,[2] Valery Ozenne,[4] Eckhard Mandelkow,[2,3] Martin Blackledge,[4] and Markus Zweckstetter[1,5,6]*

[1]Department for NMR-based Structural Biology, Max Planck Institute for Biophysical Chemistry, Göttingen, 37077, Germany
[2]German Center for Neurodegenerative Diseases (DZNE), Bonn 53175, Germany
[3]CAESAR Research Center, Ludwig-Erhard-Allee 2, Bonn 53175, Germany, and MPI for Metabolism Resesearch, Hamburg Outstation, c/o DESY, 22607 Hamburg, Germany
[4]Institut de Biologie Structurale (IBS), CEA, CNRS, University Grenoble Alpes, Grenoble 38044, France
[5]German Center for Neurodegenerative Diseases (DZNE), Göttingen 37075, Germany
[6]Department of Neurology, University Medical Center Göttingen, Göttingen 37073, Germany

Received 20 October 2015; Accepted 26 February 2016
DOI: 10.1002/pro.2911
Published online 3 March 2016 proteinscience.org

Abstract: Misfolding of the microtubule-associated protein Tau is a hallmark of Alzheimer disease and several other neurodegenerative disorders. Because of the dynamic nature of the Tau protein, little is known about the changes in Tau structure that occur during misfolding. Here we studied the structural consequences upon binding of the repeat domain of Tau, which plays a key role in pathogenic aggregation, to an aggregation enhancer. By combining NMR experiments with molecular simulations we show that binding of the aggregation enhancer polyglutamic acid remodels the conformational ensemble of Tau. Our study thus provides insight into an early event during misfolding of Tau.

Keywords: Alzheimer disease; NMR spectroscopy; Tau; protein misfolding; structure

Introduction

The microtubule-associated protein Tau plays a key role in Alzheimer disease (AD).[1] In healthy conditions, Tau binds to tubulin and microtubules, promotes tubulin polymerization and regulates microtubule dynamics in neurons.[2] However, during the course of AD, Tau misfolds and aggregates into oligomers and amyloid fibrils, which further associate into neurofibrillary tangles in the intracellular space.[1,3,4] The appearance and distribution of Tau aggregates correlates with the loss of neurons and cognitive functions in AD.[5] Insoluble aggregates of Tau contain a small β-sheet rich core surrounded by highly dynamic, unstructured regions, which appear in electron micrographs as a fuzzy coat.[6–12] Little, however, is known about the changes in Tau structure that occur at the onset of misfolding.

Increasing evidence suggests that truncated Tau, which has been cleaved by proteases and is abundant in neurofibrillary tangles, contributes to Tau-mediated neurodegeneration.[13–17] Many of the Tau fragments produced by proteases contain part of the pseudo-repeats in the C-terminal half of the protein,

Abbreviations: AD, Alzheimer disease; CD, circular dichroism; DLS, dynamic light scattering; DTT, dithiothreitol; HSQC, heteronuclear single quantum coherence; MTSL, (1-oxy-2,2,5,5-tetramethyl-d-pyrroline-3-methyl)-methanethiosulfonate; NMR, nuclear magnetic resonance; PRE, paramagnetic relaxation enhancement; Tau^{RD}, repeat domain of Tau.

Additional Supporting Information may be found in the online version of this article.

Disclosure: The authors declare no competing financial interest.

Grant sponsor: DFG (ZW 8-1 to MZ).

*Correspondence to: Markus Zweckstetter; E-mail: Markus.Zweckstetter@dzne.de

which are crucial for aggregation of Tau.[12,18,19] Important proteases are caspases, which cleave Tau at residue 421,[15] calpain,[16,20] autophagy-induced cleavage (Tau residues 258 to ~360)[19] and asparagine endopeptidase (residues 255 to 368),[13] which liberate the repeat domain for aggregation. Within the repeat domain there are two hexapeptide sequences, which establish Tau-Tau interactions,[18,21] drive aggregation of Tau via β-sheet formation,[18,22] and form the core of Tau amyloid fibrils.[7,8,11] In addition, the central domain of Tau harbors several genetic mutations, such as N279K and ΔK280, which cause hereditary frontotemporal dementia and parkinsonism linked to chromosome 17.[23] The importance of the repeat domain of Tau, Tau^{RD}, for aberrant misfolding is further supported by the interaction of a variety of aggregation inhibitors with this region.[11,12,24]

Although Tau aggregates are a pathological hallmark of several neurodegenerative diseases,[1] Tau is highly soluble in solution. This is because the Tau sequence contains only a small number of hydrophobic residues but many polar and charged amino acids.[25] Thus, additional factors are required to initiate the misfolding of Tau. Post-translational modifications such as phosphorylation have been thought to contribute,[26] but polyanionic cofactors such as heparan sulfate proteoglycans, ribonucleic acids, and acidic peptides are more potent in nucleating Tau assembly.[27,28] Indeed, neurofibrillary tangles isolated from the brains of patients with AD contain many non-protein components including glycosaminoglycans and ribonucleic acids.[28] Consistent with these findings, polyanionic cofactors promote misfolding of Tau *in vitro*.[28–30]

Insight into the structural changes that occur during misfolding of Tau is hampered by the dynamic nature of Tau: Tau belongs to the class of intrinsically disordered proteins and does not fold into a stable tertiary structure in solution.[25,31] It is therefore best described by an ensemble of conformations.[31–39] To overcome the challenges associated with the dynamic nature of Tau and obtain insight into the first steps of Tau misfolding, we combined NMR spectroscopy with computational biology. We determined an ensemble of conformations of the repeat domain of Tau, Tau^{RD} [also called K18; Fig. 1(a)], in the absence and presence of the aggregation enhancer polyglutamic acid. The conformational ensembles revealed a tightening of intramolecular interactions between the aggregation-prone regions, suggesting that this might be an important step in the misfolding of Tau.

Results

Microtubule-binding domain of tau remains monomeric in the presence of polyglutamic acid at subthreshold temperatures

Tau is an intrinsically disordered protein, which in the brain misfolds into oligomeric species and is further converted into amyloid fibrils rich in β-structure.[1] We therefore asked how the aggregation enhancer polyglutamic acid changes the structure of Tau^{RD} at 22°C, just below the critical temperature for assembly.[40] First, we tested if addition of polyglutamic acid results in the immediate formation of Tau oligomers. To this end, we analyzed Tau^{RD} in the absence and presence of a 10-fold molar excess of polyglutamic acid using DLS. Hydrodynamic radius values observed for Tau^{RD} in the absence and presence of polyglutamic acid were similar [Fig. 1(b)]. This indicates that Tau^{RD} remains predominantly monomeric upon addition of polyglutamic acid and only aggregates into oligomers and fibrils at higher temperatures and longer incubation times, consistent with the ionic nature of the interaction.[40]

Next, we analyzed the secondary structure of Tau^{RD} using CD spectroscopy [Fig. 1(c)]. Both in the absence and presence of polyglutamic acid, the CD curves showed a negative trough around 200 nm that is characteristic of random coil structure [Fig. 1(b)].[36] Although a change in the CD signal was observed between 210 and 230 nm, this is due to the contribution of polyglutamic acid[41] and does not indicate the formation of stable elements of α-helix or β-structure. Consistent with a highly dynamic nature of Tau, two-dimensional [^{1}H,^{15}N]–HSQC spectra retained low NMR signal dispersion in the presence of high concentrations of polyglutamic acid [Fig. 1(d)]. Only after incubation at 37°C for 7 days, a signature of β-structure was found by CD, indicating that amyloid fibrils had formed [Fig. 1(b)]. In contrast, NMR signal intensities remained unchanged when the NMR sample was kept for seven days without stirring at 5°C (Supporting Information Fig. S1), indicating that at best very little oligomerization occurred during the NMR measurement at low temperature.

Polyglutamic acid modulates the dynamic structure of tau

Although Tau^{RD} remained flexible in the presence of polyglutamic acid, the aggregation enhancer perturbed many of its NMR signals [Fig. 2(a)]. For the hexapeptide ^{275}VQIINK^{280} the signal intensities decreased by about 40%, while those of residues 360–362 (far away from the hexapeptide motifs) were almost unchanged [Fig. 2(b)]. The residue-specific signal broadening was caused by the exchange of Tau^{RD} residues between the free and polyglutamic acid-bound state and the associated averaging of chemical shifts. We attribute the distributed nature of signal broadening to a transient interaction of the negatively charged polyglutamic acid with positively charged Tau residues. In addition, we detected pronounced chemical shift changes upon addition of polyglutamic acid [Fig. 2(a)]. These were largest in the two hexapeptide sequences at

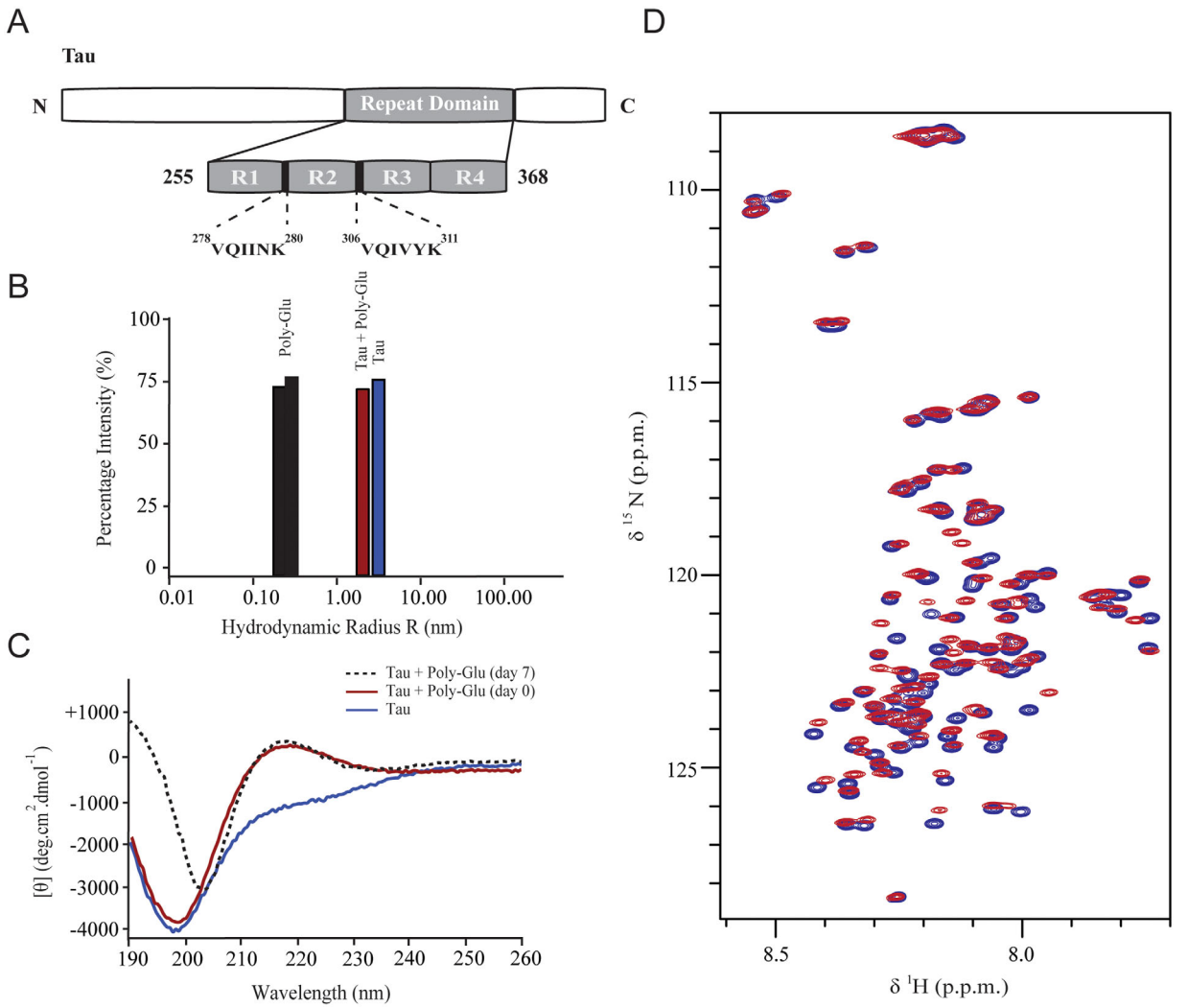

Figure 1. Structural properties of the protein Tau. (**a**) Schematic representation of full-length Tau and the repeat domain of Tau, TauRD, which is formed by four pseudo-repeat sequences (R1–R4) and comprises the amyloid-core residues of Tau. The location of the two aggregation-prone hexapeptide motifs ^{275}VQIINK^{280} and ^{306}VQIVYK^{311} is indicated. (**b**) Hydrodynamic radii of TauRD in the absence (blue) and presence of a 10-fold molar excess of polyglutamic acid (red) at 22°C, just below the critical temperature for assembly.[40] For comparison, the data of free polyglutamic acid are shown in black (0.7 ± 0.3 nm). Hydrodynamic radii as measured by DLS for TauRD were 3.4 ± 0.6 nm and 2.7 ± 0.5 nm in the absence and presence of polyglutamic acid, respectively, demonstrating a polyglutamic acid-mediated compaction of TauRD. (**c**) Far UV-CD spectra of TauRD in the absence (blue) and presence of a 10-fold molar excess of polyglutamic acid before (red) and after incubation for seven days (dotted line). The negative trough around 200 nm is characteristic of random coil structure, while the hump at ~216 nm is contributed by polyglutamic acid.[41] (**d**) Two-dimensional [^{1}H,^{15}N]–HSQC spectra of TauRD in the absence (blue) and presence (red) of a 10-fold molar excess of polyglutamic acid recorded at 5°C. The low signal dispersion shows that TauRD remains highly dynamic in the presence of polyglutamic acid.

the beginning of the repeats R2 and R3 [Fig. 2(b)], in particular for ^{275}VQIINK^{280}, consistent with previous observations.[36]

We then asked if the binding of polyglutamic acid changes the backbone conformation of TauRD. To this end, we determined carbon chemical shifts, which are sensitive probes of the local conformation in both globular and intrinsically disordered proteins.[42] Experimental δCα and δCO shift upfield in β-sheets and downfield in α-helices such that the difference between experimental chemical shift and the amino acid-specific random coil value is $\Delta\delta C < 0$ (extended structure) and $\Delta\delta C > 0$ (helical conformation), respectively. Chemical shift analysis of free TauRD showed stretches with a propensity for extended structure in the two hexapeptide sequences of R2 and R3, as well as for ^{336}QVEVKSEKLD^{345} and ^{357}LDNIT^{361}.[36] A similar pattern was observed in the presence of a 10-fold molar excess of polyglutamic acid (Supporting Information Fig. S2). Calculation of the difference between experimental δCO values in the presence and absence of polyglutamic acid showed that δCO values increased in the hexapeptide in repeat R2, but decreased at the N-

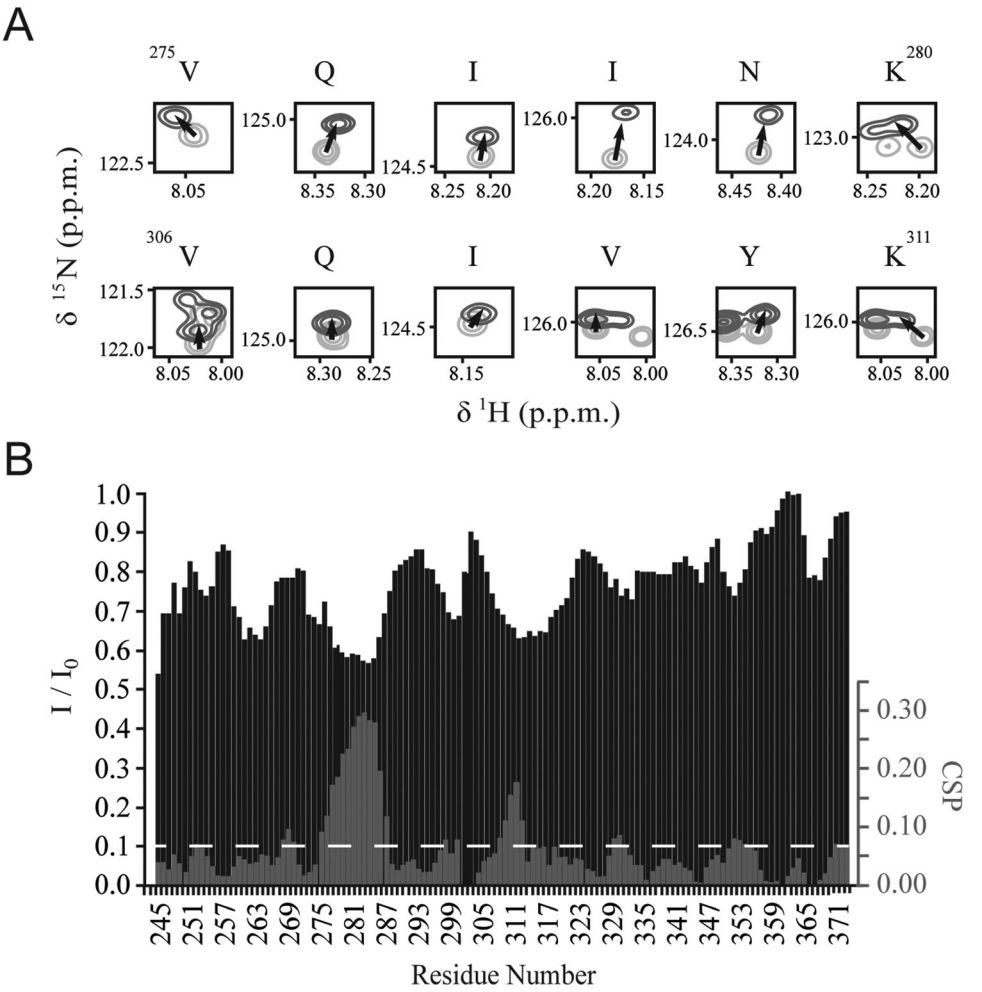

Figure 2. Polyglutamic acid binds to aggregation-prone regions of Tau. (**a**) Selected regions of 2D [^{1}H,^{15}N]–HSQC spectra of TauRD without (light gray) and with a 10-fold molar excess of polyglutamic acid (dark gray). The protein concentration was 50 μ*M*. (**b**) Residue-specific chemical shift perturbations and NMR intensity ratios in the absence I_0 and presence, I, of polyglutamic acid. The white dotted line corresponds to a threshold of 0.1. The aggregation-prone hexapeptide sequence ^{275}VQIINK^{280} in repeat R2 was most strongly perturbed by polyglutamic acid.

terminal end of R3 (Supporting Information Fig. S3). This shows that binding of polyglutamic acid slightly perturbs the local structure in Tau.

Intramolecular contacts in TauRD

Transient contacts between distant regions of the primary sequence are found in many intrinsically disordered proteins.[43–49] To obtain insight into transient contacts formed in TauRD, we made use of the high sensitivity of NMR signals to the presence of paramagnetic centers.[50] To this end, we designed four variants of TauRD, which each carry a single cysteine residue at a distinct position along the primary sequence of TauRD. The selected mutants include single-point mutations, in which one of the two native cysteine residues (C291 or C322) of Tau were substituted by alanine, as well as the variants, in which the native cysteines were replaced by alanine and a new cysteine was introduced in either position 260 or 354. Subsequently, a nitroxide spin label MTSL was covalently attached to each of the four variants.

The presence of a paramagnetic center in a protein results in enhanced relaxation of the NMR resonances, because of the dipole–dipole interaction between the unpaired electron in the paramagnetic center and the NMR-active nucleus. This broadening effect is strongly distance dependent and can reach up to 25 Å in case of MTSL. For the four MTSL-labeled variants of TauRD, we quantified paramagnetic relaxation enhancement by comparison of NMR signal intensities in 2D HSQC experiments recorded in the paramagnetic (I_{para}) and diamagnetic state (I_{dia}) (Supporting Information Fig. S4). In agreement with the $1/r^6$-dependence of the paramagnetic effect, crosspeaks of residues in direct proximity to C322 were broadened beyond detection (Supporting Information Fig. S4B). For residues slightly further away, I_{para}/I_{dia} ratios rapidly increased. The asymmetric appearance of the

broadening profile showed that residues 323–372 are in transient contact with the paramagnetic center.

Next, we analyzed the influence of the paramagnetic center at position 354 on the NMR resonances of TauRD. In this case, a strong attenuation (~40%) of the signals of residues ^{306}Val-Leu315 was observed (Supporting Information Fig. S4). In addition, signals from the first hexapeptide ^{275}VQINNK^{280} at the beginning of repeat R2 were decreased by about 10–20%. Transient interactions between distant regions in TauRD were further supported by the paramagnetic broadening profiles for the spin label at position 291: the spin label caused broadening for almost all residues in TauRD (Supporting Information Fig. S4). In particular, residues in the hexapeptide^{306}VQIVYK^{311} lost 80% of their signal intensity.

Polyglutamic acid induces specific contacts between aggregation-prone sites

The above data showed that all four repeats are in transient contact, in particular the two aggregation-prone hexapeptide sequences. We therefore asked if one of the first steps at the onset of Tau misfolding is a modulation of the network of transient long-range contacts. To address this question, we added a 10-fold molar excess of polyglutamic acid to the four variants of TauRD, which contain a single paramagnetic center (Supporting Information Fig. S4). For TauRD with the spin label at position 322, a polyglutamic acid-induced enhancement of the paramagnetic broadening of residues ^{275}VQIINK^{280} was observed. For the spin label at position 260, PRE broadening was enhanced in a larger region of the repeat domain, including residues in R2 and R3. Moreover, a slightly stronger PRE effect was found for 30 residues up- and down-stream of the spin label at position 291. The combined PRE data suggest that the conformational ensemble of the repeat domain of Tau becomes more compact in the presence of poly-glutamic acid. In agreement with a tightening of transient contacts, the DLS-detected average hydrodynamic radius of TauRD decreased from 3.4 to 2.7 nm upon addition of polyglutamic acid [Fig. 1(c)]. Notably, the NMR data show that the repeat domain of Tau remained highly dynamic in the presence of polyglutamic acid. This is critical to remember when interpreting the PRE data. When working with a stably folded protein, it is expected that PRE profiles from different MTSL sites are fully complementary, that is, when one PRE profile indicates that the distance to another residue is decreased upon some trigger, the same information should be found when the MTSL is attached to this particular residue. In contrast, when working with largely disordered proteins, which populate a large ensemble of conformations and only have transient contacts, the PRE profiles do not have to be fully

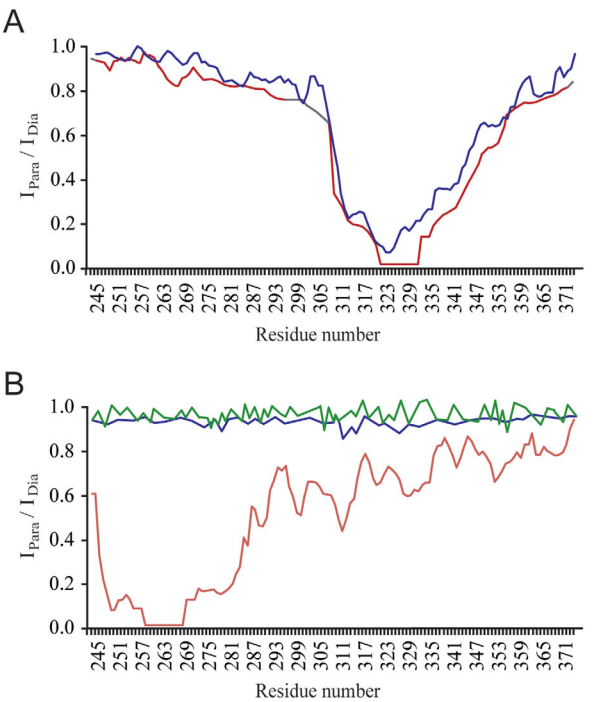

Figure 3. The intramolecular nature of the transient contacts. (**a**) Residue-specific intensity ratios between the paramagnetic and diamagnetic states of TauRD tagged with MTSL at C322. Protein concentrations were 150 μ*M* (red) and 50 μ*M* (blue). (**b**) Relative NMR signal intensities (green) in cysteine-free ^{15}N-labeled TauRD-C291A/C322A when mixed with an equal amount (100 μ*M*) of ^{14}N-containing TauRD tagged with MTSL at position 260. Intensity ratios observed after addition of a 10-fold molar excess of polyglutamic acid are shown in blue. For comparison, the PRE profile of TauRD (with the MTSL attached to position 260) in the presence of a 10-fold molar excess of polyglutamic acid is shown in red.

complementary. This is because NMR spectroscopy only reports on the average properties of a large number of molecules. Thus, different transient contacts can be present in different molecules.

Because polyglutamic acid enhances the aggregation of Tau, the observed increase in paramagnetic broadening might be caused by the formation of intermolecular contacts. To probe for the influence of intermolecular interaction on the paramagnetic broadening profile, we repeated the measurements with the paramagnetic proteins at threefold lower concentration. A reduction of the protein concentration from 150 to 50 μ*M*, however, only slightly changed the MTSL-induced broadening profile [Fig. 3(a)]. We further probed for the presence of intermolecular contacts by using a mixture of spin-labelled TauRD and a cysteine-free TauRD variant in the presence and absence of polyglutamic acid. Because only this variant was labeled with ^{15}N, paramagnetic broadening would only be observed in case of intermolecular contacts. However, no intensity reduction for the paramagnetic state was detected even after addition of a tenfold molar excess of polyglutamic

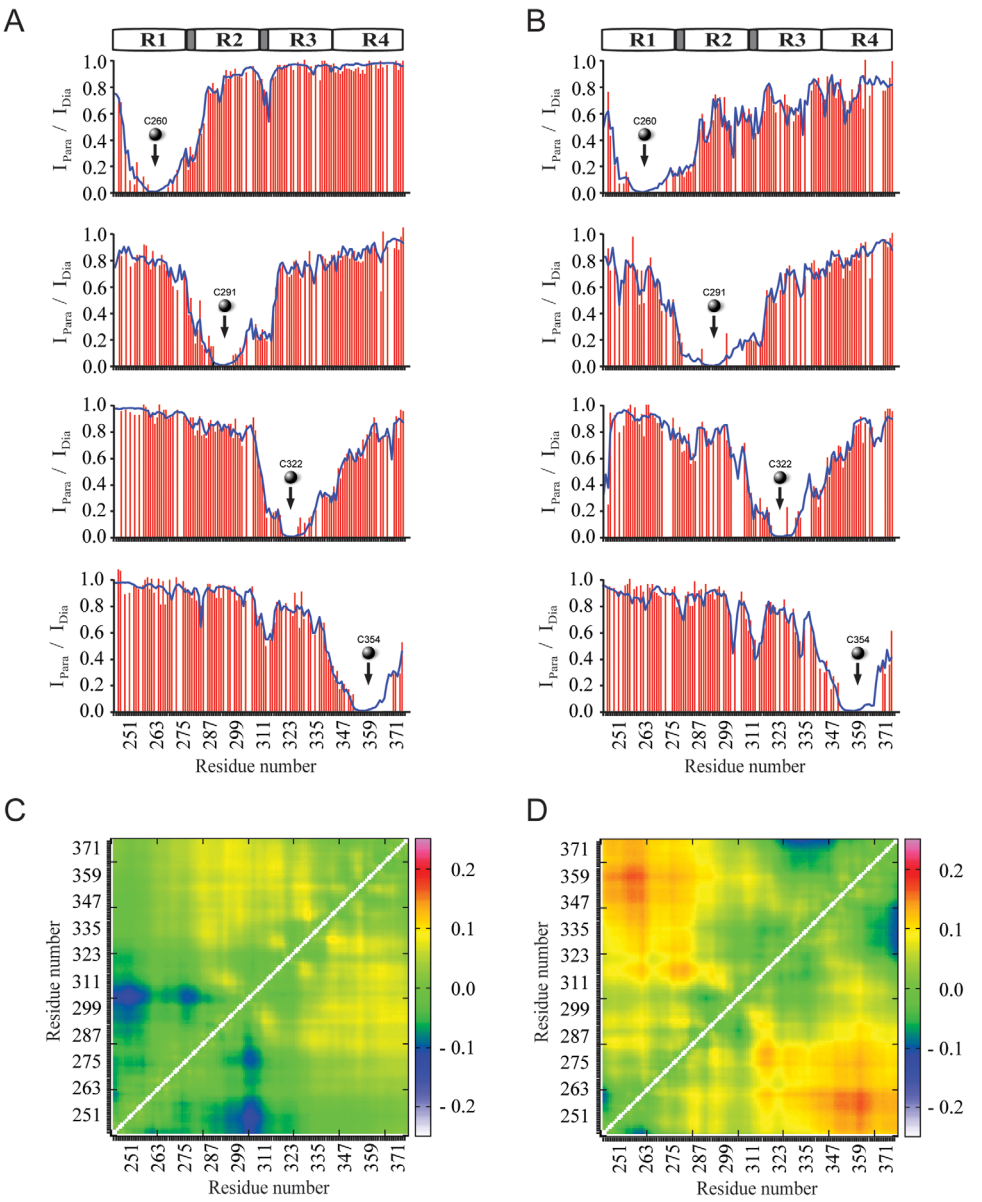

Figure 4. Conformational ensembles of the repeat domain of Tau in the absence and presence of polyglutamic acid. (**a**, **b**) Comparison of experimental PRE broadening profiles (red) with values back-calculated from molecular ensembles (blue) in the absence (a) and presence of a 10-fold molar excess of polyglutamic acid (b). The attachment sites of MTSL are indicated by arrows. (**c, d**) Distance matrices of Tau^{RD} in the absence (c) and presence of a 10-fold molar excess of polyglutamic acid (d). Contacts are plotted as $\log(d_{ij}/d_{ij,ref})$ where $d_{ij,ref}$ refers to the distance in the reference ensemble of 30,000 structures and d_{ij} refers to the distance in the ensemble selected on the basis of the experimental PREs. Each selected ensemble contained 80 structures.

acid [Fig. 3(b)]. Thus, the specific contacts induced by polyglutamic acid in Tau^{RD} are exclusively intramolecular.

Molecular ensembles at the onset of misfolding

Tau is highly dynamic and interconverts between a large number of conformations.[31] To obtain a structural view of the ensemble of conformations, which are populated in the absence and presence of polyglutamic acid, we performed statistical coil calculations under the influence of the experimentally observed paramagnetic effects. Using the ASTEROIDS approach,[51,52] ensembles of 30,000 structures were calculated for Tau^{RD}. The ensembles were optimized against the measured paramagnetic effects observed in either the absence or the presence of polyglutamic acid, resulting in 80 structures in each ensemble. Subsequently, I_{para}/I_{dia} ratios were back-calculated from the molecular ensembles and averaged over five repeat calculations. For all spin-label positions and both in the presence and absence of polyglutamic acid, the molecular ensembles accurately reproduced the experimentally observed paramagnetic effects [Fig. 4(a,b)]. This includes in

particular also the PRE profiles for MTSL positions 260 and 291, which at first sight might not be fully complementary (Supporting Information Fig. S4). The ensemble calculations unambiguously demonstrated that ensembles containing 80 conformers can fully reproduce the PRE profiles of both of these spin label positions, as well as of the spin label positions 322 and 354. This is in agreement with the dynamic nature of Tau and the fact that NMR parameters are always ensemble averages.

Next, we analyzed the selected ensembles for changes in C^{α} contact probabilities. To this end, the log of the ratio of the average distances in the ensembles of Tau^{RD} in the absence and presence of polyglutamic acid were calculated [Fig. 4(c,d)]. Comparison of the two residue-specific maps demonstrated that long-range contacts between the pseuorepeats R1 and R4 were more populated in the presence of polyglutamic acid. In addition, polyglutamic acid tightened the interaction between the aggregation-prone hexapeptide sequences (Fig. 4).

Discussion

Intrinsically disordered proteins such as Tau and α-synuclein are highly soluble due to the large number of polar and charged residues, yet their aggregation into oligomers and amyloid fibrils are intimately linked to disease. Because of the high solubility and the generally low protein concentrations in the cell, cellular factors must exist, which promote the pathogenic aggregation of these proteins. Indeed, various cellular polyanions (e.g., RNA, acidic peptides, or micelles) drastically accelerate aggregation of Tau and were found together with Tau aggregates in AD brains.[28,29] We therefore asked what the critical step in the misfolding of Tau is that occurs upon binding to an aggregation enhancer.

Using a combination of NMR spectroscopy and molecular ensemble calculations we investigated both the local and global structure of the repeat domain of Tau upon binding to polyglutamic acid. We chose polyglutamic acid for these studies, because previous work had suggested that polyglutamic acid does not immediately convert Tau into oligomers.[36] This is in contrast to the polyanion heparin, which rapidly induces the formation of Tau oligomers at the concentrations required for NMR spectroscopy.[21,36] Indeed, a variety of experimental controls performed in the current study demonstrated that the repeat domain of Tau is predominantly monomeric in the presence of polyglutamic acid, as long as the temperature is kept low (Figs. (1 and 3), and Supporting Information Fig. S1). This made it possible to specifically analyze the structural changes that occur in the repeat domain of Tau upon binding to an aggregation enhancer.

Consistent with the high abundance of positive charges in the repeat domain of Tau, the binding of polyanions preferentially occurs in this region.[36,53] The sequence-specific assignment of the backbone resonances showed chemical shift perturbation at the two hexapeptide sequences in repeats R2 and R3 (Fig. 2). This can be caused by the direct binding of polyglutamic acid, a binding-induced structural change in the repeat domain of Tau or a combination of both. Although the local structure was indeed perturbed in the presence of polyglutamic acid, changes remained small (Supporting Information Fig. S3), in agreement with circular dichroism [Fig. 1(b)] and previous studies.[36,53] Instead, some changes were induced in the transient contacts between different parts of the repeat domain of Tau (Fig. 4). In particular, contacts between the aggregation-prone hexapeptide sequences were tightened in the presence of polyglutamic acid. This resulted in an overall compaction of the repeat domain of Tau as evidenced by dynamic light scattering [Fig. 1(c)] and in agreement with single-molecule Förster resonance energy transfer measurements, which had been performed for full-length Tau in the presence of heparin.[37] Our data suggest that an important step in the misfolding of Tau is the intramolecular compaction of aggregation-prone regions of Tau. Notably, formation of an intramolecular crosslink between the two native cysteines at position 291 and 322 delays aggregation of Tau,[54] indicating that a specific conformational change triggers Tau misfolding, while disulfide bond formation locks Tau into an aggregation-incompetent state.

Materials and Methods

Sample preparation

Tau^{RD}, which corresponds to residues 244–372 of Tau [Fig. 1(a)], was expressed in *Escherichia coli* and purified as described previously.[31,36] Briefly, proteins were expressed in the vector pNG2 (Merck) in *E. coli* strain BL21(DE3). The expressed proteins were purified from bacterial extracts by making use of the heat stability of the protein and by FPLC SP-Sepharose chromatography (GE Healthcare). For uniform labeling with ^{15}N and ^{13}C isotopes, *E. coli* bacteria were grown in M9-based minimal medium containing 1 g/L of $^{15}NH_4Cl$ and 4 g/L of D-Glucose (^{13}C-6), or 1 g/L of $^{15}NH_4Cl$ alone. The cell pellets were suspended in extraction buffer (50 m*M* MES, 500 m*M* NaCl, 1 m*M* $MgCl_2$, 1 m*M* EGTA, 5 m*M* DTT, pH 6.8) complemented with protease inhibitor mix, disrupted with a French press and boiled for 20 min. The soluble extract was isolated by centrifugation, and the supernatant was dialyzed against a buffer containing 20 m*M* MES, 50 m*M* NaCl, 1 m*M* EGTA, 1 m*M* $MgCl_2$, 2 m*M* DTT, 0.1 m*M* PMSF, pH 6.8, and loaded on an FPLC SP–sepharose column. The proteins were eluted by a linear gradient of 20 m*M* MES, 1*M* NaCl, 1 m*M* EGTA, 1 m*M* $MgCl_2$,

2 m*M* DTT, 0.1 m*M* PMSF, pH 6.8. The mutations Tau^{RD}-C291A/C322A/I260C, Tau^{RD}-C322A, Tau^{RD}-C291A, and Tau^{RD}-C291A/C322A/I354C were generated using the Quick Change site-directed mutagenesis kit (Stratagene, Waldbronn, Germany) and were confirmed by DNA sequencing. NMR samples contained Tau^{RD} at a concentration of 50 μ*M* (unless mentioned otherwise), 50 m*M* phosphate buffer, pH 6.8. Polyglutamic acid (average molecular weight of 3250, mean length ~22 Glu residues) was obtained from Sigma (Sigma-Aldrich Chemie GmbH, Schnelldorf, Germany).

To label the single cysteine-containing mutants of Tau^{RD} with the nitroxide spin label (1-oxy-2,2,5,5-tetramethyl-D-pyrroline-3-methyl)-methanethiosulfonate (MTSL; Toronto Research Chemicals, Ontario, Canada), Dithiothreitol (DTT) was removed from the buffer using size-exclusion chromatography (PD-10 column; GE Healthcare, Freiburg, Germany), followed by equilibration in PBS buffer (pH 7.4). Free sulfhydryl groups were reacted with a fivefold molar excess of MTSL solubilized in ethyl acetate, at 21°C for 2.5 h. Unreacted spin label was removed using PD-10 columns equilibrated in 50 m*M* sodium phosphate buffer (pH 6.8). Spin-labeled proteins were concentrated using Amicon Ultra-15 centrifugal filters (molecular weight cutoff of 3000; Millipore, Cork, Ireland).

NMR spectroscopy

NMR experiments were recorded at 5°C on Bruker Avance 700, 800, and 900 MHz spectrometers equipped with cryogenic probes. Two-dimensional ^{1}H–^{15}N heteronuclear single quantum coherence (HSQC) spectra were recorded with 600 complex points in the indirect dimension, 32 scans per increment and spectral widths of 8389 and 1844 Hz in the ^{1}H and ^{15}N dimension, respectively (total experiment time: 9 h). Three-dimensional HNCACB and HNCO triple-resonance experiments were measured on samples containing 1 m*M* $^{15}N/^{13}C$-labeled Tau^{RD} in 50 m*M* phosphate buffer pH 6.8, 4 m*M* DTT and 10% (v/v) D_2O. 3D HNCACB spectra were recorded with 2048 [F1] × 84 [F2] × 128 [F3] complex points and 24 scans per increment with spectral widths of 7716, 1705, and 10,582 Hz in the ^{1}H, ^{15}N, and ^{13}C dimensions, respectively (total experiment time: 3 days). 3D HNCO spectra were recorded with 2048 [F1] × 100 [F2] × 100 [F3] complex points and 8 scans per increment with spectral widths of 7003, 1561, and 1233 Hz in the ^{1}H, ^{15}N, and ^{13}C dimensions, respectively (total experiment time: 3 days). NMR spectra were processed with NMRPipe[55] and analyzed using CCPN Analysis.[56] Averaged and normalized chemical shift perturbations were calculated according to $\Delta\delta_{AV}=[0.5(\delta_{Htit}-\delta_{Hwt})^2 + 0.02(\delta_{Ntit} - \delta_{Nwt})^2]^{1/2}$, where $\delta_{Hwt}/\delta_{Htit}$ and $\delta_{Nwt}/\delta_{Ntit}$ are the ^{1}H and ^{15}N chemical shifts of Tau^{RD} in the absence/presence of polyglutamic acid.

Secondary chemical shift values were calculated as the difference between measured Cα or CO chemical shifts and the empirical random coil value for the appropriate amino acid type.[57] Random coil values for histidines, glutamates, and aspartates were taken from Wishart and Sykes,[58] as the chemical shifts of these residues are particularly sensitive to pH. To estimate the secondary structure content, the observed Cα chemical shifts were normalized by the empirically determined secondary shift expected for that amino acid type in a regular secondary structure (β-sheet or α−helix) conformation,[58] summed and normalized by the number of residues in the segment.

NMR intensity ratio plots were reported with a 3-residues averaging window. Paramagnetic Relaxation Enhancement (PRE) effects of NMR signals were extracted from the peak intensity ratios between the 2D [^{1}H,^{15}N]-HSQC NMR spectra acquired in the presence of the nitroxide radical (paramagnetic state) and after addition of 2 m*M* DTT (heated to 42°C for 10 min before measurement) to the same sample. Addition of DTT cleaves the MTSL tag from the cysteine residue such that the spin label is no longer attached to the protein and the protein is in the diamagnetic state. We previously showed that oxidation of the MTSL tag by ascorbic acid gives very similar results in the case of Tau.[31] For PRE profiles, the peak intensity of every residue in the HSQC with the tag attached was divided by the peak intensity in the HSQC with the cleaved tag (PRE = I_{para}/I_{dia}). Measurements were performed in the absence and presence of a 10-fold molar excess of polyglutamic acid. To exclude intermolecular contacts as cause for PRE line-broadening, a mixture of 100 μ*M* ^{15}N-labeled Tau^{RD}-C291A/C322A mutant (i.e., without any cysteine residue) and 100 μ*M* ^{14}N-containing Tau^{RD}-C291A/C322A/I260C, which was tagged with MTSL, was measured in the presence and absence of a 10-fold molar excess of polyglutamic acid.

Ensemble calculation

The algorithm Flexible-meccano[59] was used to create explicit ensembles of molecules that sample the conformational space available to Tau^{RD} in the absence and presence of polyglutamic acid. Unbiased conformational ensembles of 30,000 structures were calculated, and effective relaxation rates for each conformer calculated in the presence of the different spin probes. MTSL side-chain flexibility was incorporated by allowing the side-chain to sample all sterically allowed rotamers, and averaging the relaxation rates of each backbone conformation. Transverse relaxation rates for each conformer were calculated and transformed into intensity ratios. The

correlation time for the electron–nuclear interaction was set to 5 ns, in broad agreement with previous studies of unfolded proteins using PREs.[50,60] Exchange between individual backbone conformers was assumed to be fast on the chemical shift and relaxation rate timescale, so that average relaxation rates were calculated over the selected ensemble. Subensembles of 200 structures were selected on the basis of agreement with respect to the experimentally measured intensity ratios using the genetic algorithm ASTEROIDS.[51]

Dynamic light scattering

Dynamic light scattering (DLS) measurements were performed at 22°C using a DynaPro Titan temperature controlled microsampler (Wyatt Technologies Corporation). Samples (10 μ*M* of Tau^{RD} in 50 m*M* phosphate buffer, pH 6.8, and 1 m*M* DTT inserted in 50 μL flow cells in the absence or presence of a 10-fold molar excess of polyglutamic acid) were illuminated with a 25 mW, 780 nm solid-state laser, and the intensity of 90° angle scattered light was measured at 4 μs intervals using a solid-state avalanche photodiode. Measurements were performed with freshly prepared samples, each experiment lasted 20 min and was repeated six times to confirm the reproducibility of the results (i.e., total of 2 h). Average values and their standard deviations were determined using the software package Dynamics 6.7.7.9.

Circular dichroism

Circular dichroism (CD) spectra of 10 μ*M* of Tau^{RD} in 50 m*M* phosphate buffer were acquired at 25°C using a Chirascan CD spectrometer (Applied Photophysics Limited) in the absence or presence of a 10-fold molar excess of polyglutamic acid. Spectra were acquired with 350 μL in a cuvette with 0.5 m*M* path cell over the range covering 190–260 nm using a 1 nm band width and a scanning speed of 20 nm/min. Five scans (measurement time for a single scan was 5 min) were averaged for each dataset and the subsequent spectra of the buffer constituents were subtracted from the protein samples. The same measurement was repeated three times using freshly prepared samples to confirm the reproducibility of the results. Data are expressed in terms of the mean residual ellipticity (θ) in [deg/(cm^2 dmol)].

ACKNOWLEDGMENT

We thank Sabrina Hübschmann for sample preparation, Christian Griesinger and Eva Mandelkow for discussions.

REFERENCES

1. Ballatore C, Lee VM, Trojanowski JQ (2007) Tau-mediated neurodegeneration in Alzheimer's disease and related disorders. Nat Rev Neurosci 8:663–672.
2. Drubin D, Kirschner M (1986) Tau protein function in living cells. J Cell Biol 103:2739–2746.
3. Haass C, Selkoe DJ (2007) Soluble protein oligomers in neurodegeneration: lessons from the Alzheimer's amyloid beta-peptide. Nat Rev Mol Cell Biol 8:101–112.
4. Duff K, Knight H, Refolo LM, Sanders S, Yu X, Picciano M, Malester B, Hutton M, Adamson J, Goedert M, Burki K, Davies P (2000) Characterization of pathology in transgenic mice over-expressing human genomic and cDNA tau transgenes. Neurobiol Dis 7:87–98.
5. Braak H, Braak E (1991) Neuropathological staging of Alzheimer-related changes. Acta Neuropathol 82:239–259.
6. Bibow S, Mukrasch MD, Chinnathambi S, Biernat J, Griesinger C, Mandelkow E, Zweckstetter M (2011) The dynamic structure of filamentous tau. Angew Chem Int Ed Engl 50:11520–11524.
7. Daebel V, Chinnathambi S, Biernat J, Schwalbe M, Habenstein B, Loquet A, Akoury E, Tepper K, Muller H, Baldus M, Griesinger C, Zweckstetter M, Mandelkow E, Vijayan V, Lange A (2012) beta-Sheet core of Tau paired helical filaments revealed by solid-state NMR. J Am Chem Soc 134:13982–13989.
8. Andronesi OC, von Bergen M, Biernat J, Seidel K, Griesinger C, Mandelkow E, Baldus M (2008) Characterization of Alzheimer's-like paired helical filaments from the core domain of tau protein using solid-state NMR spectroscopy. J Am Chem Soc 130:5922–5928.
9. Berriman J, Serpell LC, Oberg KA, Fink AL, Goedert M, Crowther RA (2003) Tau filaments from human brain and from in vitro assembly of recombinant protein show cross-beta structure. Proc Natl Acad Sci USA 100:9034–9038.
10. Margittai M, Langen R (2004) Template-assisted filament growth by parallel stacking of tau. Proc Natl Acad Sci USA 101:10278–10283.
11. Wischik CM, Novak M, Edwards PC, Klug A, Tichelaar W, Crowther RA (1988) Structural characterization of the core of the paired helical filament of Alzheimer disease. Proc Natl Acad Sci USA 85:4884–4888.
12. von Bergen M, Barghorn S, Muller SA, Pickhardt M, Biernat J, Mandelkow EM, Davies P, Aebi U, Mandelkow E (2006) The core of Tau-paired helical filaments studied by scanning transmission electron microscopy and limited proteolysis. Biochemistry 45:6446–6457.
13. Zhang Z, Song M, Liu X, Kang SS, Kwon IS, Duong DM, Seyfried NT, Hu WT, Liu Z, Wang JZ, Cheng L, Sun YE, Yu SP, Levey AI, Ye K (2014) Cleavage of tau by asparagine endopeptidase mediates the neurofibrillary pathology in Alzheimer's disease. Nat Med 20:1254–1262.
14. Garcia-Sierra F, Mondragon-Rodriguez S, Basurto-Islas G (2008) Truncation of tau protein and its pathological significance in Alzheimer's disease. J Alzheimers Dis 14:401–409.
15. Gamblin TC, Chen F, Zambrano A, Abraha A, Lagalwar S, Guillozet AL, Lu M, Fu Y, Garcia-Sierra F, LaPointe N, Miller R, Berry RW, Binder LI, Cryns VL (2003) Caspase cleavage of tau: linking amyloid and neurofibrillary tangles in Alzheimer's disease. Proc Natl Acad Sci USA 100:10032–10037.
16. Wang Y, Garg S, Mandelkow EM, Mandelkow E (2010) Proteolytic processing of tau. Biochem Soc Trans 38:955–961.

17. Wang Y, Mandelkow E (2012) Degradation of tau protein by autophagy and proteasomal pathways. Biochem Soc Trans 40:644–652.
18. von Bergen M, Friedhoff P, Biernat J, Heberle J, Mandelkow EM, Mandelkow E (2000) Assembly of tau protein into Alzheimer paired helical filaments depends on a local sequence motif ((306)VQIVYK(311)) forming beta structure. Proc Natl Acad Sci USA 97: 5129–5134.
19. Wang YP, Biernat J, Pickhardt M, Mandelkow E, Mandelkow EM (2007) Stepwise proteolysis liberates tau fragments that nucleate the Alzheimer-like aggregation of full-length tau in a neuronal cell model. Proc Natl Acad Sci USA 104:10252–10257.
20. Saito K, Elce JS, Hamos JE, Nixon RA (1993) Widespread activation of calcium-activated neutral proteinase (calpain) in the brain in Alzheimer disease: a potential molecular basis for neuronal degeneration. Proc Natl Acad Sci USA 90:2628–2632.
21. Peterson DW, Zhou H, Dahlquist FW, Lew J (2008) A soluble oligomer of tau associated with fiber formation analyzed by NMR. Biochemistry 47:7393–7404.
22. Goux WJ (2002) The conformations of filamentous and soluble tau associated with Alzheimer paired helical filaments. Biochemistry 41:13798–13806.
23. Goedert M, Spillantini MG (2000) Tau mutations in frontotemporal dementia FTDP-17 and their relevance for Alzheimer's disease. Biochim Biophys Acta 1502: 110–121.
24. Akoury E, Pickhardt M, Gajda M, Biernat J, Mandelkow E, Zweckstetter M (2013) Mechanistic basis of phenothiazine-driven inhibition of Tau aggregation. Angew Chem Int Ed Engl 52:3511–3515.
25. Weingarten MD, Lockwood AH, Hwo SY, Kirschner MW (1975) A protein factor essential for microtubule assembly. Proc Natl Acad Sci USA 72:1858–1862.
26. Iqbal K, Liu F, Gong CX, Alonso Adel C, Grundke-Iqbal I (2009) Mechanisms of tau-induced neurodegeneration. Acta Neuropathol 118:53–69.
27. Friedhoff P, von Bergen M, Mandelkow EM, Davies P, Mandelkow E (1998) A nucleated assembly mechanism of Alzheimer paired helical filaments. Proc Natl Acad Sci USA 95:15712–15717.
28. Goedert M, Jakes R, Spillantini MG, Hasegawa M, Smith MJ, Crowther RA (1996) Assembly of microtubule-associated protein tau into Alzheimer-like filaments induced by sulphated glycosaminoglycans. Nature 383:550–553.
29. Paudel HK, Li W (1999) Heparin-induced conformational change in microtubule-associated protein Tau as detected by chemical cross-linking and phosphopeptide mapping. J Biol Chem 274:8029–8038.
30. Wilson DM, Binder LI (1995) Polymerization of microtubule-associated protein tau under near-physiological conditions. J Biol Chem 270:24306–24314.
31. Mukrasch MD, Bibow S, Korukottu J, Jeganathan S, Biernat J, Griesinger C, Mandelkow E, Zweckstetter M (2009) Structural polymorphism of 441-residue tau at single residue resolution. PLoS Biol 7:e34.
32. Schwalbe M, Ozenne V, Bibow S, Jaremko M, Jaremko L, Gajda M, Jensen MR, Biernat J, Becker S, Mandelkow E, Zweckstetter M, Blackledge M (2014) Predictive atomic resolution descriptions of intrinsically disordered hTau40 and alpha-synuclein in solution from NMR and small angle scattering. Structure 22:238–249.
33. Bibow S, Ozenne V, Biernat J, Blackledge M, Mandelkow E, Zweckstetter M (2011) Structural impact of proline-directed pseudophosphorylation at AT8, AT100, and PHF1 epitopes on 441-residue tau. J Am Chem Soc 133:15842–15845.
34. Smet C, Leroy A, Sillen A, Wieruszeski JM, Landrieu I, Lippens G (2004) Accepting its random coil nature allows a partial NMR assignment of the neuronal Tau protein. Chembiochem 5:1639–1646.
35. Eliezer D, Barre P, Kobaslija M, Chan D, Li X, Heend L (2005) Residual structure in the repeat domain of tau: echoes of microtubule binding and paired helical filament formation. Biochemistry 44:1026–1036.
36. Mukrasch MD, Biernat J, von Bergen M, Griesinger C, Mandelkow E, Zweckstetter M (2005) Sites of tau important for aggregation populate {beta}-structure and bind to microtubules and polyanions. J Biol Chem 280:24978–24986.
37. Elbaum-Garfinkle S, Rhoades E (2012) Identification of an aggregation-prone structure of tau. J Am Chem Soc 134:16607–16613.
38. Nath A, Sammalkorpi M, DeWitt DC, Trexler AJ, Elbaum-Garfinkle S, O'Hern CS, Rhoades E (2012) The conformational ensembles of alpha-synuclein and tau: combining single-molecule FRET and simulations. Biophys J 103:1940–1949.
39. Bernado P, Mylonas E, Petoukhov MV, Blackledge M, Svergun DI (2007) Structural characterization of flexible proteins using small-angle X-ray scattering. J Am Chem Soc 129:5656–5664.
40. Friedhoff P, Schneider A, Mandelkow EM, Mandelkow E (1998) Rapid assembly of Alzheimer-like paired helical filaments from microtubule-associated protein tau monitored by fluorescence in solution. Biochemistry 37:10223–10230.
41. Rinaudo M, Domard A (1976) Circular dichroism studies on alpha-l-glutamic acid oligomers in solution. J Am Chem Soc 98:6360–6364.
42. Dyson HJ, Wright PE (2004) Unfolded proteins and protein folding studied by NMR. Chem Rev 104:3607–3622.
43. Jensen MR, Zweckstetter M, Huang JR, Blackledge M (2014) Exploring free-energy landscapes of intrinsically disordered proteins at atomic resolution using NMR spectroscopy. Chem Rev 114:6632–6660.
44. Fisher CK, Stultz CM (2011) Constructing ensembles for intrinsically disordered proteins. Curr Opin Struct Biol 21:426–431.
45. Mittag T, Kay LE, Forman-Kay JD (2010) Protein dynamics and conformational disorder in molecular recognition. J Mol Recognit 23:105–116.
46. Allison JR, Varnai P, Dobson CM, Vendruscolo M (2009) Determination of the free energy landscape of alpha-synuclein using spin label nuclear magnetic resonance measurements. J Am Chem Soc 131:18314–18326.
47. Xiang S, Gapsys V, Kim HY, Bessonov S, Hsiao HH, Mohlmann S, Klaukien V, Ficner R, Becker S, Urlaub H, Luhrmann R, de Groot B, Zweckstetter M (2013) Phosphorylation drives a dynamic switch in serine/arginine-rich proteins. Structure 21:2162–2174.
48. Mittag T, Forman-Kay JD (2007) Atomic-level characterization of disordered protein ensembles. Curr Opin Struct Biol 17:3–14.
49. Wright PE, Dyson HJ (1999) Intrinsically unstructured proteins: re-assessing the protein structure–function paradigm. J Mol Biol 293:321–331.
50. Gillespie JR, Shortle D (1997) Characterization of long-range structure in the denatured state of staphylococcal nuclease. II. Distance restraints from paramagnetic relaxation and calculation of an ensemble of structures. J Mol Biol 268:170–184.

51. Salmon L, Nodet G, Ozenne V, Yin G, Jensen MR, Zweckstetter M, Blackledge M (2010) NMR characterization of long-range order in intrinsically disordered proteins. J Am Chem Soc 132:8407–8418.
52. Nodet G, Salmon L, Ozenne V, Meier S, Jensen MR, Blackledge M (2009) Quantitative description of backbone conformational sampling of unfolded proteins at amino acid resolution from NMR residual dipolar couplings. J Am Chem Soc 131:17908–17918.
53. Sibille N, Sillen A, Leroy A, Wieruszeski JM, Mulloy B, Landrieu I, Lippens G (2006) Structural impact of heparin binding to full-length Tau as studied by NMR spectroscopy. Biochemistry 45:12560–12572.
54. Schweers O, Mandelkow EM, Biernat J, Mandelkow E (1995) Oxidation of cysteine-322 in the repeat domain of microtubule-associated protein tau controls the *in vitro* assembly of paired helical filaments. Proc Natl Acad Sci USA 92:8463–8467.
55. Delaglio F, Grzesiek S, Vuister GW, Zhu G, Pfeifer J, Bax A (1995) NMRPipe: a multidimensional spectral processing system based on UNIX pipes. J Biomol NMR 6:277–293.
56. Vranken WF, Boucher W, Stevens TJ, Fogh RH, Pajon A, Llinas M, Ulrich EL, Markley JL, Ionides J, Laue ED (2005) The CCPN data model for NMR spectroscopy: development of a software pipeline. Proteins 59: 687–696.
57. Schwarzinger S, Kroon GJ, Foss TR, Chung J, Wright PE, Dyson HJ (2001) Sequence-dependent correction of random coil NMR chemical shifts. J Am Chem Soc 123: 2970–2978.
58. Wishart DS, Sykes BD (1994) Chemical shifts as a tool for structure determination. Methods Enzymol 239: 363–392.
59. Bernado P, Blanchard L, Timmins P, Marion D, Ruigrok RW, Blackledge M (2005) A structural model for unfolded proteins from residual dipolar couplings and small-angle X-ray scattering. Proc Natl Acad Sci USA 102:17002–17007.
60. Parigi G, Rezaei-Ghaleh N, Giachetti A, Becker S, Fernandez C, Blackledge M, Griesinger C, Zweckstetter M, Luchinat C (2014) Long-range correlated dynamics in intrinsically disordered proteins. J Am Chem Soc 136:16201–16209.